Pressure effect studies in molecular magnetism

2004 J. Phys.: Condens. Matter 16 S1087

(http://iopscience.iop.org/0953-8984/16/14/019)

INSTITUTE OF PHYSICS PUBLISHING JOURNAL OF PHYSICS: CONDENSED MATTER

J. Phys.: Condens. Matter **16** (2004) S1087–S1108 PII: S0953-8984(04)74877-8

Pressure effect studies in molecular magnetism

Philipp Gütlich[1], **Ana B Gaspar**[1], **Vadim Ksenofontov**[1] **and Yann Garcia**[2]

[1] Institut für Anorganische Chemie und Analytische Chemie, Johannes Gutenberg Universität, Staudinger Weg 9, D-55099 Mainz, Germany
[2] Département de Chimie, Université Catholique de Louvain, Place Louis Pasteur 1, B-1348 Louvain-la-Neuve, Belgium

E-mail: guetlich@uni-mainz.de

Received 21 January 2004
Published 26 March 2004
Online at stacks.iop.org/JPhysCM/16/S1087
DOI: 10.1088/0953-8984/16/14/019

Abstract

We report on temperature dependent magnetic susceptibility and Mössbauer effect studies of the influence of hydrostatic pressure (up to 1.2 GPa) on dynamic electronic structure phenomena in 3d transition metal coordination compounds. The systems under investigation are mononuclear spin crossover compounds of iron (II) and chromium (II), dinuclear complexes of iron (II) exhibiting coexistence of intramolecular antiferromagnetic coupling and thermal spin crossover, 1D, 2D and 3D polynuclear spin crossover complexes of iron (II), a valence tautomeric system of cobalt (II) showing a thermal transition from a high spin [Co^{II} (semiquinone)] to a low spin [Co^{II} (catecholate)] species on lowering the temperature and a photomagnetically active Prussian blue type system with temperature- and pressure induced electron transfer. It is demonstrated that pressure effect studies can be very helpful in elucidating the mechanisms and cooperative interactions of solid state compounds with electronic bistability.

Dedicated to Professor Peter Jutzi on the occasion of his 65th birthday.

1. Introduction

Current developments in advanced electronic and photonic technologies require new functional materials exhibiting bistability behaviour at the molecular scale [1, 2]. In fact, the design and synthesis of molecules or molecular assemblies for information processing is one of the most appealing aims of modern molecular chemistry. Whatever the final goal, a fundamental underlying concept is that of bistability: the ability of the molecular system to exist in two different electronic states and the same temperature. The reversible change between low spin (LS) and high spin (HS) states driven by variation of temperature and/or pressure or also by slight irradiation, mainly observed in pseudo-octahedral iron (II) coordination complexes, has

been up to now one of the best examples of molecular bistability [3–5]. At the molecular scale, spin crossover (SCO) in the Fe(II) compounds corresponds to an intra-ionic transfer of two electrons between the t_{2g} and e_g orbitals, $(t_{2g})^4(e_g)^2 \leftrightarrow (t_{2g})^6(e_g)^0$, accompanied by a change of spin state, $S = 2 \leftrightarrow S = 0$. The $^5T_{2g}$ state corresponding to $(t_{2g})^4(e_g)^2$ is the ground state only up to a critical value of the ligand field strength of $10Dq$ equal to the spin pairing energy. Above this value the $^1A_{1g}$ LS state corresponding to $(t_{2g})^6(e_g)^0$ is lower in the energy than the HS state and thus becomes the ground state [3a]. In the HS state, the antibonding e_g orbitals are doubly occupied, and consequently the Fe–donor atom bonds are longer than in the LS state by about 0.20 Å. This increase of the molecule size when passing from the LS to the HS state plays a crucial role in the cooperative mechanism of SCO giving rise to abrupt transitions and hysteresis at a macroscopic scale. For instance, the magnetic and optical properties may switch sharply in a very small range of temperature and/or pressure for cooperative transitions [5, 6]. Due to this particularity, the SCO phenomenon has been considered one of the most interesting examples of molecular switching. The condition to achieve in order to observe the phenomenon of spin transition is that the zero-point energy between the two states, $\Delta E^0_{HL} = E^0_{HS} - E^0_{LS}$, has to be of the order of the thermal energy, $k_B T$. In this case, all molecules will be in the LS state at very low temperatures or higher pressures, whereas at elevated temperatures or lower pressures an entropy-driven almost quantitative population of the HS state will occur. In general, spin transition is a well-established phenomenon and some examples of SCO complexes exhibiting abrupt spin transitions at room temperature, with broad thermal hysteresis as well as an associated thermochromic effect (necessary conditions for display devices), have been reported. Nevertheless, while barochromic properties of SCO materials have been recognized from the outset of SCO research, pressure studies remained less explored than investigations of thermally induced spin transitions, mainly due to experimental difficulties. There was a revival of interest in the effect of pressure on SCO complexes during the last decade involving studies using either hydrostatic cells adapted to magnetic susceptibility [7], Mössbauer [8], optical absorption [9] and reflectivity detection methods [10] or diamond anvil cells (DACs) in conjunction with methods of detection such as IR [11], EXAFS [12] and x-ray diffraction [13] techniques. The DAC technique is not well adapted for studying the spin transition process because pressure loops are difficult to record in the most interesting pressure range (<1.0 GPa) and problems of non-hydrostaticity are likely to arise from pressure gradients in the cell. Hydrostatic pressure cells adapted for the other techniques have been used to study the effect of pressure on the spin transition temperature, thermal and pressure induced hysteresis cycles, the crystal structure and the relaxation process. The first part of the present article is devoted to studies of the effect of pressure on SCO materials of different dimensionality carried out in our laboratory using hydrostatic cells developed for magnetic susceptibility and Mössbauer measurements, illustrating how pressure effect studies can help in understanding the nature of cooperative interactions. The second part of this contribution deals with pressure effect studies on another dynamic electronic structure phenomenon, the valence tautomerism in a cobalt catecholate complex and in a Prussian blue type system.

2. Experimental section

2.1. Materials

The compounds have been synthesized and characterized according to procedures described elsewhere[3].

[3] The syntheses of the compounds studied in the present article are described in [25, 26, 27, 7f, 6d, 46, 48, 49, 52, 53].

2.2. Magnetic susceptibility measurements under hydrostatic pressure

The variable-temperature magnetic susceptibility measurements were performed using a PAR 151 Foner type magnetometer equipped with a cryostat operating at 1 T in the temperature range 2–300 K and a Quantum Design MPMS2 SQUID susceptometer at 1 T and 1.8–300 K. The hydrostatic pressure cell made of hardened beryllium bronze with silicon oil as the pressure transmitting medium operates in the pressure range 1 bar $< P <$ 13 kbar and has been described elsewhere [14]. Hydrostaticity was established during our earlier studies of SCO compounds. The cylindrically shaped powder sample holder dimensions are 1 mm in diameter and 5–7 mm in length. The pressure was measured using the pressure dependence of the superconducting transition temperature of a built-in pressure sensor made of high purity tin. Experimental data were corrected for diamagnetism using Pascal's constants.

2.3. Mössbauer spectroscopy under hydrostatic pressure

^{57}Fe Mössbauer spectra were recorded using a conventional constant-acceleration spectrometer and a helium bath cryostat. Powder samples were measured in a Mössbauer pressure cell made of hardened beryllium bronze equipped with windows made of B_4C and with silicon oil as the pressure transmitting medium. The construction enables hydrostatic pressure measurements to be carried out up to 15 kbar in the temperature range 2–350 K. The Mössbauer pressure cell was calibrated using FeF_3 in accordance with published results [15]. The Recoil 1.02 Mössbauer Analysis Software was used to fit the experimental spectra [16]. Isomer shift values are quoted relative to α-Fe at 293 K.

3. The effect of pressure in Fe(II) spin crossover complexes

3.1. Mononuclear Fe(II) spin crossover complexes

Most iron (II) SCO compounds are constituted by mononuclear species with the $[FeN_6]$ core. Among them, the complexes of formula $[Fe(L)_2(NCS)_2]$, where L stands for a bidentate α-diimine ligand, represent one of the most extensively studied families [17–24]. They display a wide range of SCO behaviour from gradual to abrupt transitions, even with broad thermal hysteresis loops. In this section we illustrate the effect of pressure on the following examples of different SCO behaviours: an abrupt spin transition, a gradual one and a pressure induced spin transition in a paramagnetic compound. For this purpose, we have chosen the following systems: $[Fe(phen)_2(NCS)_2]$ (phen: 1,10-phenanthroline) (1) [25], $[Fe(PM\text{-}Aza)_2(NCS)_2]$ (PM-Aza: (N-(2′-piridylmethylen)-4-azophenyl aniline)) (2) [26] and $[Fe(abpt)_2(NCS)_2]$ (abpt: 4-amino-3,5-bis(pyridin-2-yl)-1,2,4-triazole) (3) [27] (figure 1). The two former compounds reveal an abrupt and a gradual spin transitions, respectively, at ambient pressure, whereas the third one is in the HS state over the whole range of temperatures under study.

3.1.1. [Fe(phen)$_2$ (NCS)$_2$] polymorph II (1). The $\chi_M T$ versus T plots of 1 at different pressures, χ_M being the molar magnetic susceptibility and T the temperature, are shown in figure 2. At ambient pressure the transition curve is extremely steep with $T_{1/2} = 177$ K. The presence of the temperature hysteresis width $\sim$2 K and the value of the residual HS fraction ($\widetilde{=}$17%) are in agreement with published data [28]. As pressure is increased, the transition curve moves upwards with an average rate 220 K GPa^{-1}. At $P = 0.17$ GPa and higher pressures the hysteresis disappears and transition curves become gradual. At $P = 0.57$ GPa the sample is mostly in the LS state; however, the residual HS fraction below the transition remains practically constant under pressure. This observation is in line with the results found in [29],

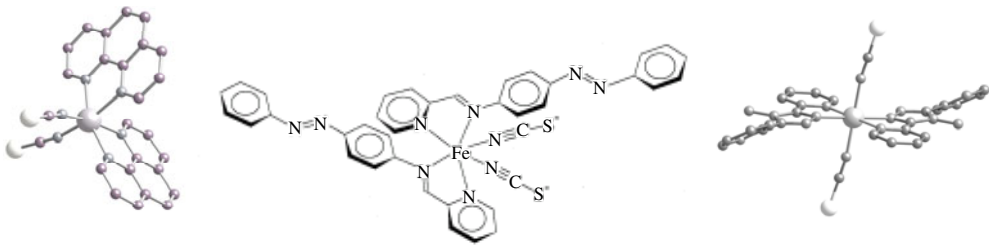

Figure 1. Molecular structures of the compounds $[Fe(phen)_2(NCS)_2]$ (1) (left), $[Fe(PM\text{-}Aza)_2(NCS)_2]$ (2) (centre), $[Fe(abpt)_2(NCS)_2]$ (3) (right).

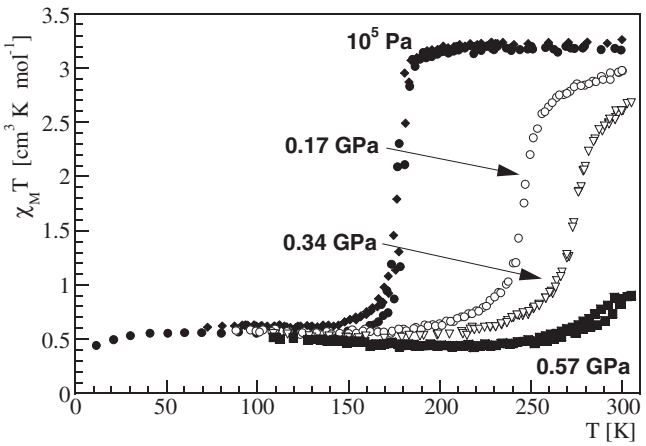

Figure 2. $\chi_M T$ versus T plots of $[Fe(phen)_2(NCS)_2]$ at different pressures.

where conservation of the space group during the SCO transition under pressure up 1.0 GPa has been reported and has stressed the role of the structure as a decisive factor influencing the completeness of SCO transition in 1. A progressive decrease of the pressure influence on the transition temperature (41.0 K GPa^{-1} at 0.17 GPa, 18.0 K GPa^{-1} at 0.34 GPa, 15.0 K GPa^{-1} at 0.57 GPa) points to a steric hindrance, which can be a decisive factor preventing the complete HS $\rightarrow$ LS transformation in 1.

3.1.2. [Fe(PM-Aza)$_2$(NCS)$_2$](2). For the mononuclear compound 2, γ_{HS} (HS molar fraction) versus T at ambient pressure decreases continuously down to about 5% as T is lowered from room temperature down to 5 K corresponding to a gradual and nearly complete spin transition. The conversion temperatures are $T_{1/2}\downarrow = 186$ K and $T_{1/2}\uparrow = 192$ K in the cooling and warming modes, respectively (figure 3). An increase of pressure shifts the transition temperature upwards and decreases the slope of the transition curve; at 0.25 GPa, $T_{1/2}$ is around 210 K, and at 1.08 GPa, $T_{1/2}$ is far above room temperature. Indeed, an increase of hydrostatic pressure stabilizes the LS state, which possesses a smaller molecular volume. It should be noted that there is linear behaviour of the pressure dependence of $T_{1/2}$ for the spin conversion of 2. The slope of the $T_{1/2}$ versus P straight line, $dT_{1/2}/dP = 16$ K GPa^{-1}, is very close to that observed for the mononuclear compounds $[Fe(2\text{-pic})_3]Cl_2 \cdot EtOH$ (2-pic = 2-picolylamine) [30] and $[Fe(abpt)_2(NCS)_2]$ where $dT_{1/2}/dP = 15$ and 17.6 K GPa^{-1}, respectively.

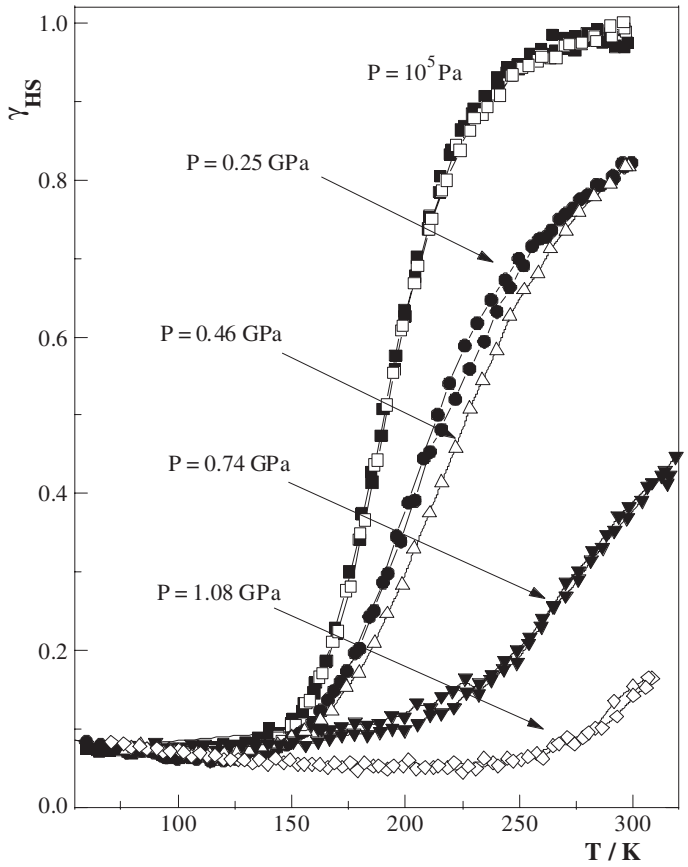

Figure 3. γ_{HS} versus T plots of [Fe(PM-Aza)$_2$(NCS)$_2$] at different pressures.

3.1.3. [Fe(abpt)$_2$ (NCS)$_2$] polymorph B (3). Figure 4 shows the temperature dependence of the $\chi_M T$ product for 3 at different pressures. At room temperature and at atmospheric pressure $\chi_M T$ is equal to 3.68 cm^3 K mol^{-1} which is in the range of the values expected for an iron (II) ion in the HS state. As the temperature is lowered, $\chi_M T$ practically remains constant; the decrease of $\chi_M T$ at temperatures below 25 K corresponds to the occurrence of zero-field splitting of the HS iron (II) ions. This behaviour persists as pressure is increased up to 0.44 GPa, where an incomplete thermal SCO appears around $T_{1/2} = 65$ K. This $T_{1/2}$ value is one of the lowest transition temperatures observed for an iron (II) SCO compound. It is likely that to reach completeness the slow kinetics is blocking the HS $\leftrightarrow$ LS equilibrium and prevents the spin transition due to the low temperatures involved in the spin transition of 3 at 0.44 GPa. A relatively sharp spin transition takes place at $T_{1/2} = 106$, 152 and 179 K, as pressure attains 0.56, 0.86 and 1.05 GPa, serially. In the slow cooling and heating modes with the rate 0.1 K min^{-1} providing thermodynamic equilibrium conditions, the transitions are accompanied by a 2 K wide thermal hysteresis at all pressures studied. Noteworthy is the linear behaviour of the pressure dependence of $T_{1/2}$ for the spin conversion of 3. The slope of the $T_{1/2}$ versus P straight line, $dT_{1/2}/dP = 17.6$ K GPa^{-1}, is very close to that observed for the mononuclear compound [Fe(2-pic)$_3$]Cl$_2$ EtOH (2-pic = 2-picolylamine) [30] where $dT_{1/2}/dP = 15$ K GPa^{-1}.

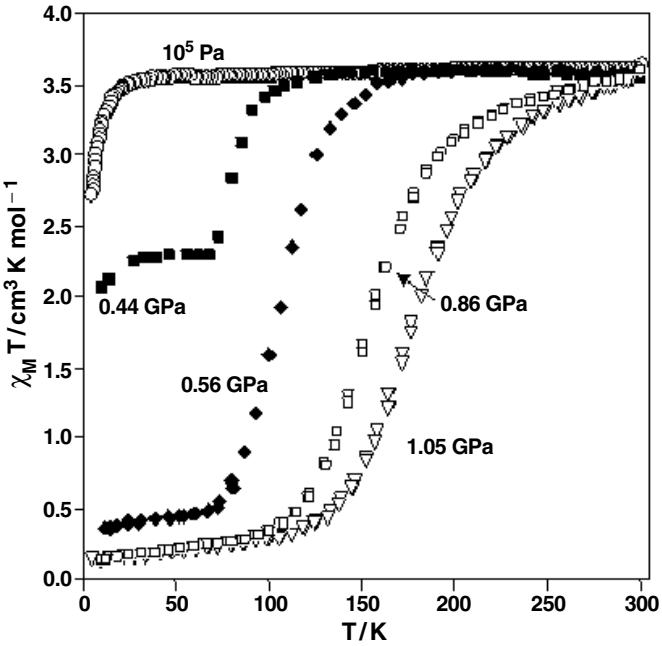

Figure 4. $\chi_M T$ versus T plots of [Fe(abpt)$_2$(NCS)$_2$] at different pressures.

The above described pressure influence on the abrupt and gradual transitions can be qualitatively interpreted on the basis of the phenomenological theory of phase transitions in SCO systems [31]. It predicts that hydrostatic pressure transforms a discontinuous spin transition accompanied by hysteresis to a transition of continuous type. Indeed, we observed this behaviour in studying the compound 1. In the framework of this theory the slope of the spin transition curve decreases under pressure and $T_{1/2}$ shifts upwards. The thermal dependence of γ_{HS} under pressure for compound 2 demonstrates these features. The pressure studies on compound 3 demonstrate the possibility to 'fine tune' the crystal field strength and thereby induce a thermal spin transition in a paramagnetic compound in a controlled way. The application of pressure turns out to be equivalent to creating 'chemical pressure', also called image pressure, by diluting the Fe(II) SCO compound isostructurally with a transition metal of different ionic radius. Extensive studies in the metal dilution effect have been reported and the results have served as the basis for the development of the model of elastic interactions and lattice expansion [3].

3.2. Dinuclear Fe(II) spin crossover complexes

The design and synthesis of polynuclear SCO complexes have represented an alternative strategy for exploring cooperativity [32]. Moreover, new kinds of SCO regimes related to the nuclearity of the system are expected. Closely associated with this strategy, there emerged the idea of combining different electronic properties such as magnetic exchange and spin transitions in the same molecule and system. A first step along this line aiming to afford a multiproperty material began with the class of 2,2′-bipyrimidine (bpym)-bridged iron (II) dinuclear compounds.

The series of compounds {[Fe(L)(NCX)$_2$]$_2$(bpym)}, where L is bpym (2,2′-bipyrimidine) or bt (2,2′-bithiazoline) and X is S or Se, comprises four complexes, two of which, (bpym,

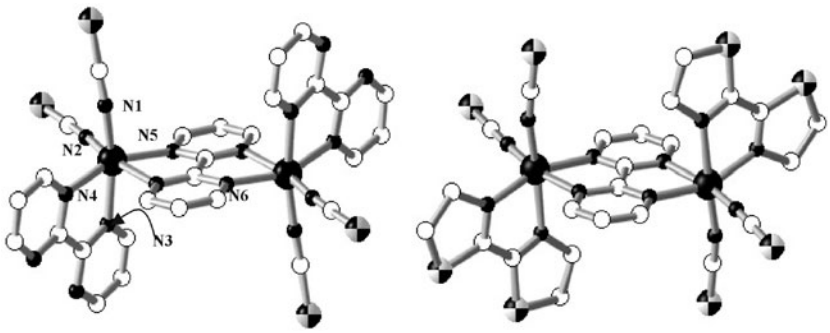

Figure 5. The molecular structure of {[Fe(bpym)$(NCS)_2]_2$(bpym)} together with the corresponding atom numbering (left) and that of {[Fe(bt)$(NCS)_2]_2$(bpym)} (right).

S) and (bt, S), have been characterized by means of x-ray single-crystal diffraction. The centrosymmetric dinuclear units {[Fe(L)$(NCS)_2]_2$(bpym)}, where L = bpym [33] or bt [34], are shown in figure 5. Each iron (II) atom is surrounded by two NCS^- anions in *cis* positions, two nitrogen atoms of the bridging bpym ligand, and the remaining positions are occupied by the peripheral bpym or bt ligands. The $[FeN_6]$ chromophore is rather distorted with Fe–N bond distances characteristic of an iron (II) ion in the HS state.

No thermal spin transition is observed for the iron (II) complex denoted as (bpym, S) over the whole range of temperature (see the next section). At first sight this is a rather unexpected result as the iron (II) environment in the dinuclear compound is close to that in $[Fe(bipy)_2(NCS)_2]$ [35]. The average Fe–N bond distances are however noticeably greater for (bpym, S). In contrast, the iron (II) complex denoted as (bt, S), which shows shorter Fe–N bond distances than (bpym, S), undergoes a complete spin transition [36]. The remaining members of this family, (bpym, Se) and (bt, Se), also undergo spin transition, but their crystal structures have not yet been solved. However, structural information on these compounds has been obtained using x-ray absorption techniques (EXAFS) at 300 and 77 K. The EXAFS data afforded a rather satisfactory description of the iron (II) coordination core both in the HS and in the LS states of these compounds [37].

The magnetic behaviour of this series at ambient pressure is depicted in figure 6. As stated before, (bpym, S) does not display thermally induced spin conversion, but exhibits intramolecular antiferromagnetic coupling between the two iron (II) ions through the bpym bridge ($J = -4.1$ cm^{-1}, $g = 2.18$). When thiocyanate is replaced by selenocyanate the resulting (bpym, Se) derivative shows an abrupt spin transition in the 125–115 K temperature region with a small hysteresis loop of 2.5 K width (see figure 6). Only 50% of the iron (II) atoms undergo spin transition. The decrease of the $\chi_M T$ values at lower temperatures is due to the occurrence of zero-field splitting of the $S = 2$ state (see below). The magnetic properties of (bt, S) and (bt, Se) are similar to one another and show a complete spin transition with the remarkable feature that it takes place in two steps centred at 197 and 163 K for (bt, S) and at 265 and 223 K for (bt, Se). In both cases, the plateau corresponds approximately to 50% spin conversion.

These macroscopic steps, also detected by means of Mössbauer spectroscopy and calorimetric measurements, were interpreted in terms of a microscopic two-step transition between the three possible spin pairs of each individual dinuclear molecule [36]:

$$[HS–HS] \leftrightarrow [HS–LS] \leftrightarrow [LS–LS].$$

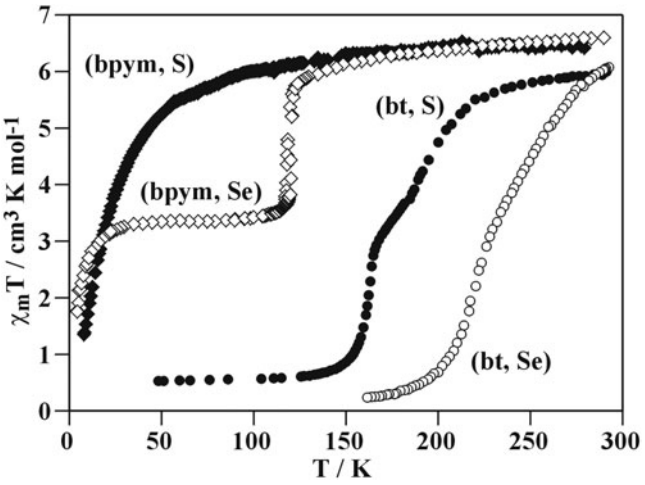

Figure 6. The temperature dependence of $\chi_M T$ for {[Fe(L)(NCX)$_2$]$_2$(bpym)} (L = bpym and X = S(bpym, S) or Se(bpym, Se) and L = bt and X = S(bt, S) or Se(bt, Se)).

The stabilization of the [HS–LS] mixed-spin pair results from a synergistic effect of intramolecular and cooperative intermolecular interactions (see below).

The pressure dependence of the thermal variation of $\chi_M T$ has proved to be a useful diagnostic probe for showing that the formation of [HS–LS] spin pairs is not fortuitous but that they are the preferentially formed species in the dinuclear type complexes [38]. It is shown next that application of external hydrostatic pressure can help to unravel features of this whole class of compounds, which can usually be revealed by variation of chemical composition.

It has already been shown that increase in hydrostatic pressure favours the LS state in mononuclear complexes, and there is no reason to expect a different behaviour for dinuclear systems. Two members of the {[Fe(L)(NCX)$_2$]$_2$bpym} family are particularly suitable candidates in this regard: (bpym, S) and (bpym, Se). Figure 7 displays the thermal dependence of $\chi_M T$ at different pressures. At ambient pressure, and over the whole temperature range, (bpym, S) contains only the antiferromagnetically coupled [HS–HS] pairs (figure 7(a)). Coexistence of antiferromagnetic coupling and SCO in (bpym, S) clearly follows from magnetic susceptibility measurements at $P = 0.63$ GPa. When the pressure is increased to 0.63 GPa a partial conversion from 100% [HS–HS] to 55% [HS–LS] species takes place. The incompleteness of spin conversion is due to the fact that at low temperatures the spin conversion is so slow that the HS state becomes metastable. Thus antiferromagnetically coupled [HS–HS] pairs and [HS–LS] uncoupled pairs become coexistent in (bpym, S) at 0.63 GPa, as reflected in the thermal dependence of $\chi_M T$. Finally, for $P = 0.89$ GPa the total conversion to [HS–LS] pairs is accomplished. It is worth noting that, at this pressure, (bpym, S) undergoes a similar [HS–HS] $\leftrightarrow$ [HS–LS] spin transition at $T_{1/2} \approx 150$ K as in (bpym, Se) at ambient pressure. The effect of pressure on the thermal dependence of the spin state of (bpym, Se) seems to be a decrease in the degree of cooperativity (as can be seen from the more gradual $\chi_M T$ function as compared to that under ambient pressure) and a shift of $T_{1/2}$ towards higher temperatures for pressures up to 0.45 GPa (figure 7(b)). For higher pressures, a second transition appears in addition to the former, due to the onset of thermal SCO in the second metal centre. Between 0.72 and 1.03 GPa a two-step SCO function is observed.

As mentioned above, the particular characteristic of the SCO process in dinuclear compounds is the appearance of a plateau in the spin transition curve. From the analysis

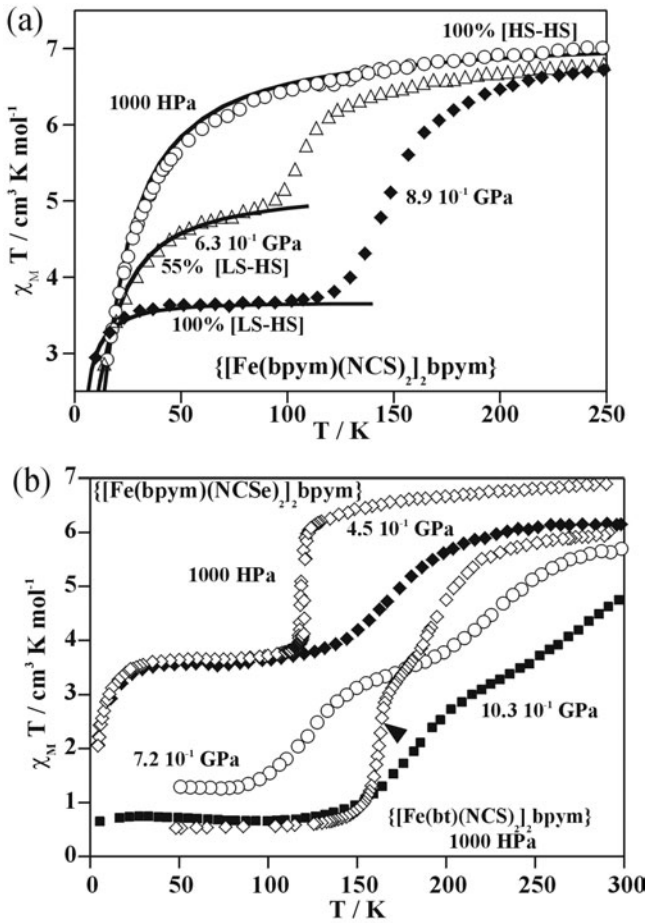

Figure 7. The temperature dependence of $\chi_M T$ for {[Fe(bpym)$(NCS)_2]_2$(bpym)} at different pressures (a). The solid curves, together with estimated concentrations of [HS–LS] and [HS–HS] species, correspond to calculations using the appropriate Hamiltonian. The temperature dependence of $\chi_M T$ for {[Fe(bpym)$(NCSe)_2]_2$(bpym)} at different pressures (b). The magnetic behaviour of {[Fe(bt)$(NCS)_2]_2$(bpym)} at ambient pressure has also (1000 hPa) been included for comparison.

of the results of the pressure experiments, it is inferred that the plateau results from successive SCO in the two metal centres, leading first to the formation of relatively stable [HS–LS] pairs and then, above a critical pressure, to the formation of [LS–LS] pairs on further lowering of the temperature. The intermolecular interactions between [HS–LS] pairs lead to domains that contribute to the stability of the crystal lattice. Indeed, in the absence of intermolecular interactions, the increase of pressure should decrease the size of the HS fraction. The pressure induced low temperature state of (bpym, S), consisting almost entirely of the [HS–LS] units, is stable at least up to 1.1 GPa. For (bpym, Se), a pressure of 0.45 GPa shifts $T_{1/2}$ by about 50 K upwards without increasing the size of the LS fraction. Only at higher pressures does the second step appear for this derivative. These experimental data underline the role of intermolecular interactions, particularly short range competing with omnipresent long range interactions, in the stabilization of the hypothetical 'checkerboard-like' structure consisting of [HS–LS] units as proposed by Spiering *et al* [39].

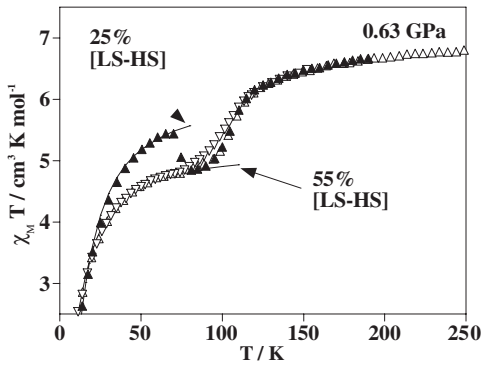

Figure 8. The temperature dependence of $\chi_M T$ for {[Fe(bpym)$(NCS)_2]_2$(bpym)} (bpym, S) under hydrostatic pressure of 0.63 GPa. A sample was cooled slowly from 300 to 4.2 K with a cooling rate of 2 K min^{-1} (open triangles). Thermal quenching experiment: the sample under pressure was cooled rapidly from 300 to 5 K with a cooling rate of about 100 K min^{-1} and then warmed slowly up to 300 K (filled triangles). After quenching a substantial fraction of the HS centres did not convert to the LS state and showed magnetic coupling in the metastable [HS–HS] pairs. Thermal relaxation to the equilibrium state takes place at about 70 K.

In order to investigate the competition between magnetic interaction and spin transition in (bpym, S) quenching experiments have been performed at 0.63 GPa. Figure 8 displays the magnetic behaviour of the quenched sample at increasing temperatures. It can be inferred from the thermal dependence of $\chi_M T$ that [HS–HS] entities can be frozen in as a metastable state at low temperatures. Heating the sample above about 60 K leads to re-formation of the stable state, which, in this temperature regime, consists mostly of [HS–LS] dinuclear species. Two main factors, namely, antiferromagnetic intramolecular interactions and elastic interactions, are believed to play an important role in the stabilization of the metastable state. Considering the low value of $J \approx -4.1$ cm^{-1} of the former in comparison with the decay temperature of $T \approx 60$ K and the unusually slow kinetics of the relaxation to the stable state, as compared to the relatively fast kinetics of spin transitions taking place at higher temperature, one can conclude that the relaxation is an essentially thermally activated process and that the crystal lattice is substantially involved. It is the structural rearrangement, associated with the spin changing process, that is responsible for the trapping of the [HS–HS] metastable species and not the magnetic interactions. If the magnetic interactions were responsible, the dynamics of the relaxation to the stable state would be much faster. In other words, elastic interactions rather than magnetic coupling drive the transformations of [HS–HS] $\leftrightarrow$ [HS–LS] under pressure.

3.3. 1D, 2D and 3D Fe(II) polymeric spin crossover complexes

The number of polymeric iron (II) SCO compounds reported up to now remains small. Most of them incorporate multidentate *N*-donor heterocyclic bridging ligands such as 1,2,4-triazole, 1-R-tetrazole, polypyridine-like derivatives as well as tetracyanometallate or dicyanometallate complex ligands [32]. These compounds generally exhibit abrupt spin transitions with hysteresis effects whose amplitude strongly depends on the nature of the molecular bridge between iron (II) sites. In this section, we review the behaviour under pressure of the spin transition of a selection of 1D, 2D and 3D polymeric iron (II) compounds.

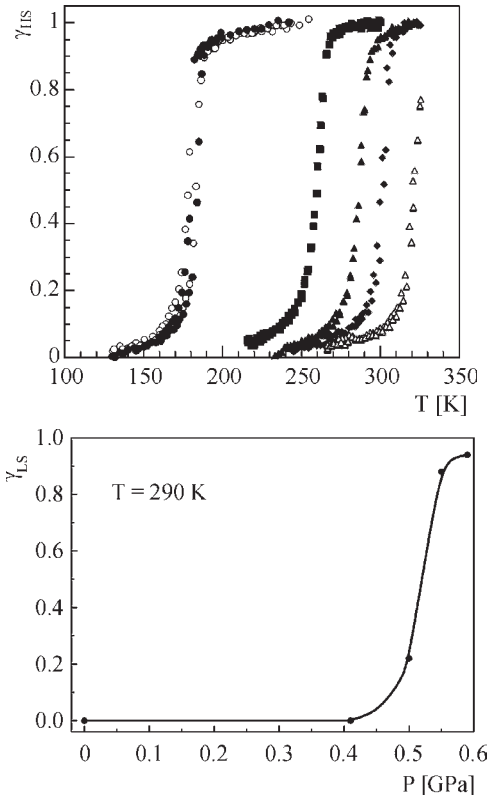

Figure 9. Top: a γ_{HS} versus T plot for [Fe(hyptrz)$_3$](4-chlorophenylsulfonate)$_2\cdot H_2O$ at different pressures. (●, $P = 10^5$ Pa; ■, $P = 0.41$ GPa; ▲, $P = 0.5$ GPa; ♦, $P = 0.53$ GPa; △, $P = 0.59$ GPa; ○, $P = 10^5$ Pa after releasing the pressure). Bottom: a γ_{LS} versus P plot for [Fe(hyptrz)$_3$](4-chlorophenylsulfonate)$_2\cdot H_2O$ at 290 K.

3.3.1. 1D chain compounds. Iron (II) 4R-1,2,4-triazole polymeric chains belong to one of the most investigated families of SCO compounds, presumably due to their potential for being incorporated in memory devices and displays. Towards this end, spin transition materials showing wide bistability domains around room temperature along with thermochromic behaviour are currently being sought [5]. [Fe(4-R-1,2,4-triazole)$_3$](anion)$_2\cdot nH_2O$ is made up of linear chains in which the adjacent iron (II) ions are linked by three *N*1,*N*2-1,2,4-triazole ligands. The non-coordinated species such as counter-anions and water molecules are localized between the chains. In these polymeric compounds, the molecular bridge is sufficiently rigid to allow an efficient transmission of cooperative effects. Consequently, abrupt spin transitions with broad thermal hysteresis loops have been observed [5]. Several approaches aiming to tune the SCO behaviour towards room temperature have been followed including the use of an external pressure [6d, 7f, 40].

Figure 9 shows the temperature dependence of the HS molar fraction for [Fe(hyptrz)$_3$](4-chlorophenylsulfonate)$_2\cdot H_2O$ (hyptrz = 4-(3′-hydroxypropyl)-1,2,4-triazole) at different pressures up to nearly 0.6 GPa [7f]. At 10^5 Pa, a very steep and complete spin transition is observed with a hysteresis loop of width ∼5 K ($T_{1/2}\downarrow = 178$ K and $T_{1/2}\uparrow = 183$ K). As the pressure increases, the spin transition curves are shifted upwards to room temperature. The profiles of the curves remain essentially unchanged with the steepness retained at all pressures.

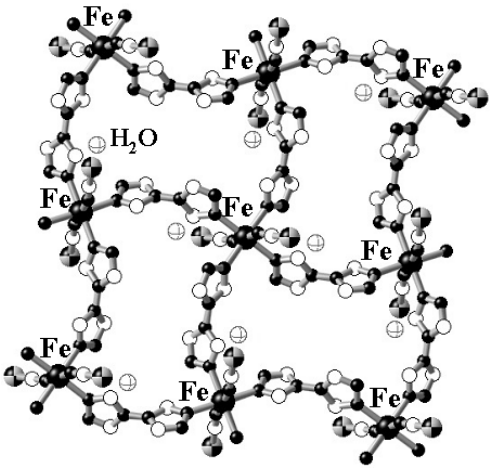

Figure 10. A representative fragment of the layered structure of $[Fe(btr)_2(NCS)_2]\cdot H_2O$.

The spin transition is observed at 260 K under 0.41 GPa, at 286 K under 0.5 GPa, at 301 K under 0.53 GPa, and at 324 K under 0.59 GPa. Interestingly, the hysteresis width reveals a non-monotonic character under pressure. It first diminishes and is no longer observed at 0.41 GPa before reappearing at a constant value of ∼5 K above 0.5 GPa. On release of the pressure, the same magnetic behaviour as observed at 10^5 Pa was obtained. Figure 9 also shows the pressure dependence of the LS fraction, γ_{LS}, of $[Fe(hyptrz)_3](4\text{-chlorophenylsulfonate})_2\cdot H_2O$. A very steep HS → LS transition is observed at room temperature around ∼0.6 GPa accompanied by a colour change from white to deep purple. This property could be used for an application such as in a pressure sensor or display [41].

This magnetic behaviour under pressure contrasts with the one observed for mononuclear SCO compounds with a systematic flattening of the spin transition curves together with a variation in the hysteresis width with increasing pressure [7a, 42]. This lends support to the assertion that cooperative interactions are confined within the Fe(II) triazole chain for this compound. Thus a change in external pressure has an effect on the SCO behaviour comparable to a change in internal electrostatic pressure due to anion–cation interactions. Both lead to considerable shifts in transition temperatures without significant influence on the hysteresis width [7f]. This behaviour under pressure appears to be a general trend for 1D polymeric chain compounds with 4-R-1,2,4-triazole as ligands. Indeed, a similar shift of the hysteresis loop upwards to room temperature was observed for the polymeric chain compound $[Fe(hyetrz)_3](3\text{-nitrophenylsulfonate})_2$ (hyetrz = 4-2′-hydroxyethyl-1,2,4-triazole) [6d]. Several theoretical models have been developed to predict such SCO behaviour of 1D chain compounds under pressure [43–45].

The magnetic properties of the HS iron (II) chain compound $[Fe(bpym)(NCS)_2]$ have also been investigated under pressure. As a result, a spin transition was induced under ∼1.2 GPa involving about 50% of iron (II) ions as found for the dinuclear compound $[Fe(bpym)(NCS)_2]_2$bpym [38].

3.3.2. 2D and 3D polymeric compounds. $[Fe(btr)_2(NCS)_2]\cdot H_2O$ (btr = 4,4′-bis-1,2,4-triazole) is a 2D polymeric SCO compound [46] which has become a model material in SCO research. The crystal structure obtained at room temperature reveals that each iron ion is

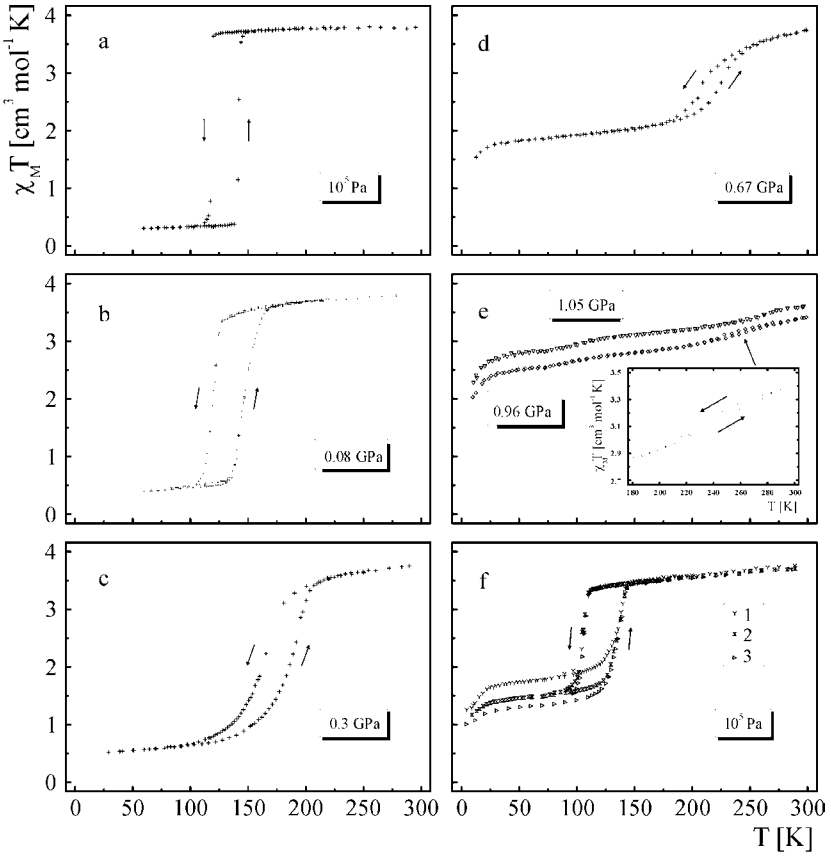

Figure 11. $\chi_M T$ versus T plots for $[Fe(btr)_2(NCS)_2]\cdot H_2O$ under different pressure up to 1.05 GPa.

bridged by one $N1,N1'$ coordinating btr ligand defining an infinite stack of layered grids. Two thiocyanate anions in apical positions complete the coordination sphere of iron (II) (figure 10). Non-coordinated water molecules are linked by hydrogen bonding to the peripheral nitrogen atoms of the triazole. The layers are connected by means of van der Waals forces and weak hydrogen bond bridges involving the water molecules [46].

$[Fe(btr)_2(NCS)_2]\cdot H_2O$ undergoes a complete spin transition centred at ∼133 K with a hysteresis loop of width 23 K under ambient pressure with $T_{1/2}\downarrow = 121$ K and $T_{1/2}\uparrow = 144$ K (figure 11). At 0.08 GPa, the hysteresis loop broadens and becomes asymmetric. Interestingly, $T_{1/2}\downarrow$ is not modified, whereas $T_{1/2}\uparrow$ is slightly shifted to higher temperature. At 0.3 GPa the spin transition curves move upwards and flatten and the hysteresis width decreases. Also a noticeable fraction of iron (II) ions remaining in the HS state over the whole temperature range (∼8%) are detected. At 0.67 GPa, the hysteresis loop is now shifted to around 215 K and its width decreases to 19 K. A pronounced increase of the residual HS iron (II) sites is observed with around 50% of the molecules being in the HS state at low temperatures. When the pressure is further increased, the spin transition becomes increasingly gradual and incomplete. At 1.05 GPa, a totally HS curve is observed. Thus, application of hydrostatic pressure surprisingly results in stabilization of the HS state, contrary to the normal expectation that pressure should stabilize the LS state due to its smaller volume. On release of the pressure, the HS state

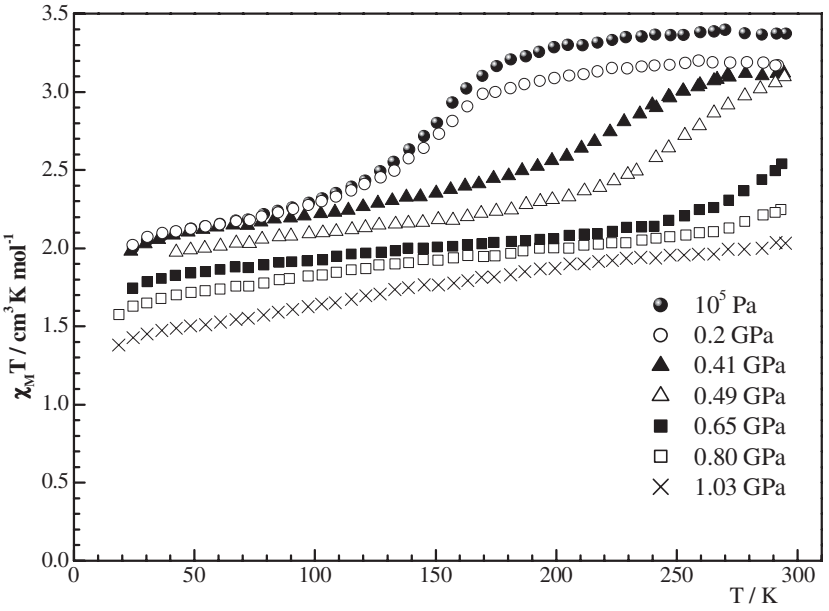

Figure 12. $\chi_M T$ versus T plots for $[Fe(btr)_3][Fe(btr)_2(H_2O)_2](BF_4)_4$ over the temperature range 20–300 K and at different pressures up to 1.03 GPa.

remains partially trapped. Indeed, an incomplete spin transition involving ∼50% of iron (II) ions which is shifted by 7 K to lower temperatures ($T_{1/2}\uparrow = 137$ K and $T_{1/2}\downarrow = 105$ K) and whose hysteresis becomes larger (32 K) with respect the one obtained before applying any pressure, is observed [7d].

LIESST experiments have been performed on this compound at 10 K. These have shown that after thermal relaxation of the metastable HS state obtained by light switching, a pure LS state was observed in contrast to the pressure experiment results. This different behaviour suggests that pressure leads to a structural modification that is presumably responsible for the pressure induced HS state [7d]. Another possibility would be to consider that under pressure some water molecules enter the coordination sphere of iron (II) and thus establish a weaker ligand field strength leading to the observation of the HS state. ^{57}Fe Mössbauer spectroscopy under pressure and structural studies are necessary to clarify this unexpected magnetic behaviour.

The magnetic properties of $[Fe(btr)_3][Fe(btr)_2(H_2O)_2](BF_4)_4$ were investigated up to 1.03 GPa [47]. This 2D or 3D compound reveals a gradual SCO behaviour involving ∼50% of HS iron (II) ions at ambient pressure with $T_{1/2} \sim 150$ K (figure 12). At 0.2 GPa, the SCO curve follows the same pathway as for 10^5 Pa except over the temperature range 160–298 K for which a slight lowering of $\chi_M T$ is observed. Upon increasing pressure, the SCO curve flattens and is shifted upwards to higher temperatures. The residual fraction of HS iron (II) remains constant up to 0.41 GPa, after which a pronounced decrease is observed over the whole temperature range. At 1.03 GPa, a large fraction of HS Fe(II) ions are still present. No stepwise spin transition is observed under pressure as for $[Fe(bpym)(NCSe)_2]_2bpym$ [38]. This magnetic behaviour under pressure can be explained by the presence of FeN_6 and FeN_4O_2 sites as the FeN_6 sites are responsible for the SCO behaviour whereas the FeN_4O_2 sites remains HS throughout the whole temperature range [47].

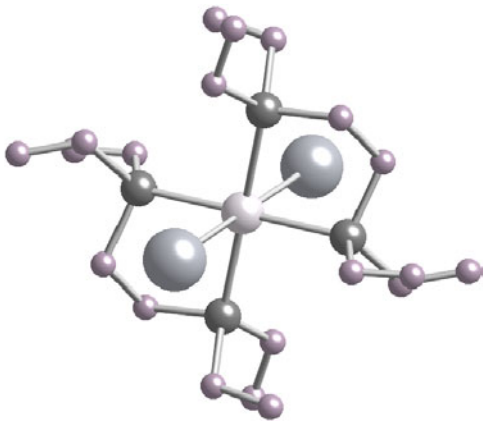

(a)

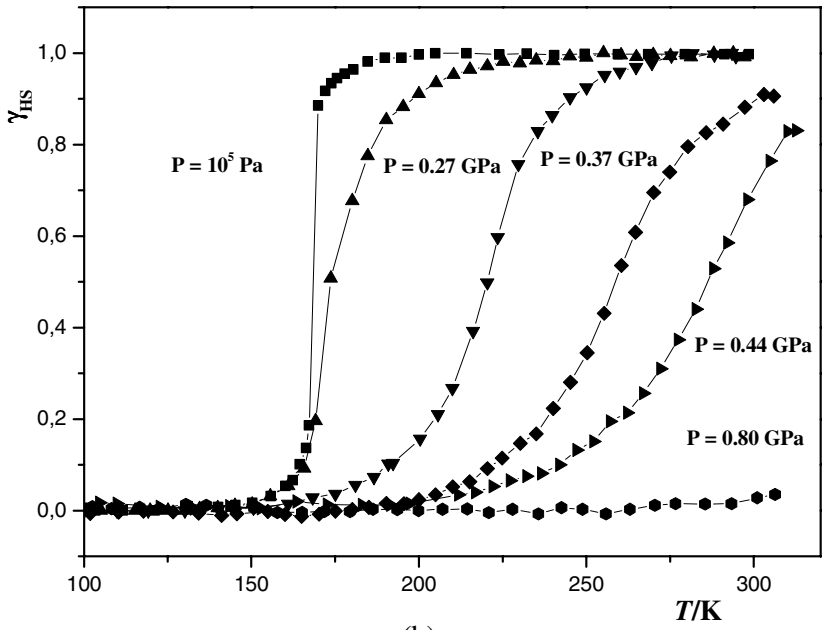

(b)

Figure 13. Molecular structure (a) and $\chi_M T$ versus T plots at different pressures for the spin crossover complex $[CrI_2(depe)_2]$ (b).

(This figure is in colour only in the electronic version)

The magnetic properties of the 3D SCO compounds $\{Fe(L)_2[Ag(CN)_2]_2\}$ with L = bipy = 4,4′-bipy and L = bpe = bis-pyridyl-ethylene have also been investigated under pressure [48]. $\{Fe(bipy)_2[Ag(CN)_2]_2\}$ is HS over the whole temperature range under ambient pressure. Application of 0.48 GPa induces an incomplete SCO behaviour with $T_{1/2} \sim 150$ K. At 0.7 GPa, the compound becomes essentially LS at room temperature. This spin transition induced by pressure at room temperature is found to be reversible. A similar magnetic behaviour under pressure is found for $\{Fe(bpe)_2[Ag(CN)_2]_2\}$ [48].

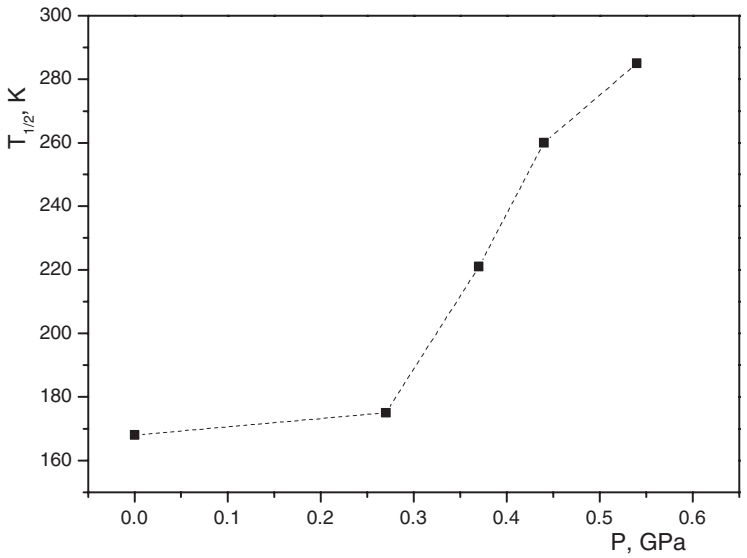

Figure 14. The pressure dependence of the spin transition temperature $T_{1/2}$ of $[CrI_2(depe)_2]$.

4. The effect of pressure on the mononuclear spin crossover complex $[CrI_2\ (depe)_2]$

The phenomenon of thermal SCO is found most often in mononuclear compounds of iron (II), iron (III), cobalt (II), and is rather rare in complexes of other transition elements. The first thermal spin crossover in chromium (II) compounds was reported by Halepoto *et al* in 1989 [49]. The ground state of the divalent chromium ion in a weak octahedral ligand field is ^5E_g with $S = 2$. In strong octahedral ligand fields, the ground state is $^3T_{1g}$ with low spin behaviour and $S = 1$. The chromium (II) compound of the present study, bis[1,2-bis(diethylphosphino)ethane]diiodochromium (II) (hereafter $[CrI_2(depe)_2]$), has a *trans* configuration (figure 13(a)) and at ambient pressure exhibits a very sharp spin transition with $T_{1/2} = 169$ K without noticeable thermal hysteresis [49]. A magnetic susceptibility study under pressure shows a progressive increase of $T_{1/2}$ and a decrease of the transition steepness with increasing pressure (figure 13(b)). Application of pressure of 0.8 GPa transforms the compound entirely to the LS state at ambient temperature. Qualitatively, one can interpret the behaviour of the transition curves under pressure on the grounds of mean field theory [50]. In mean field approximation the pressure dependence of the spin transition temperature obeys the Clausius–Clapeyron relation:

$$\frac{\partial T_{1/2}}{\partial P} = \frac{\Delta V}{\Delta S_{\mathrm{HL}}}.$$

This relation reflects essentially the pressure dependence of the transition temperature $T_{1/2}$ on the volume change ΔV. The dependence of $T_{1/2}$ versus pressure for $[CrI_2(depe)_2]$ shows strong non-linearity (figure 14). A detailed interpretation of this is not possible without knowledge of the thermal and pressure dependences of the elementary cell volume of $[CrI_2(depe)_2]$. One cannot exclude the possibility of a small change of the elementary cell volume of $[CrI_2(depe)_2]$ in the pressure range up to $\approx$0.3 GPa. The big iodide ions are expected to be more easily compressible than the phosphorus atoms and, as a result, should lead to an anisotropic volume change on application of pressure. A quantitative interpretation of the influence of pressure on the SCO behaviour of this chromium compound, particularly the pressure dependence of

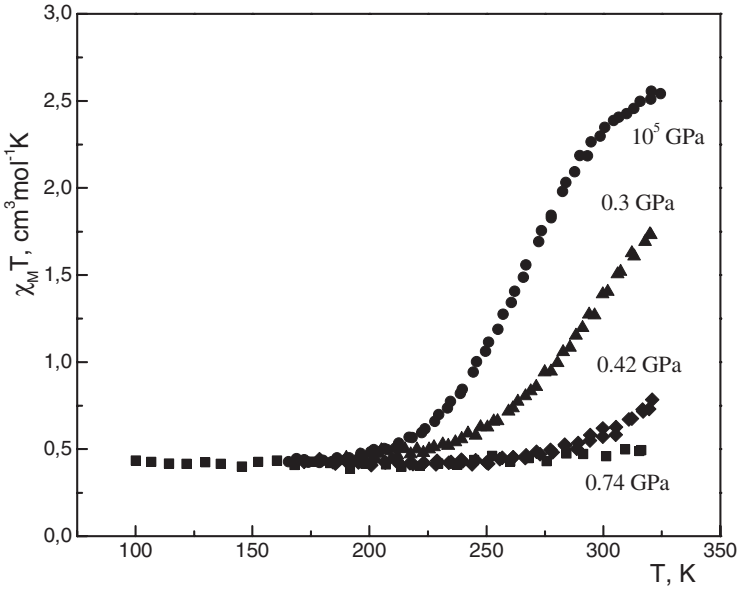

Figure 15. $\chi_M T$ versus T plots at different pressures for [Co(cth)(phendiox)]$PF_6 \cdot H_2O$.

the transition temperature $T_{1/2}$ as indicated by the experimental data in figure 14, is only possible with a detailed crystallographic study of $[CrI_2(depe)_2]$ under pressure and at variable temperatures.

5. The effect of pressure on valence tautomeric systems

5.1. The O-dioxolene adduct of a cobalt–tetraazamacrocycle complex

The phenomenon of temperature induced valence tautomerism in cobalt complexes has been well established in the literature [51]. In these systems, a thermally induced intramolecular one-electron transfer takes place between the catecholato ligand and the LS cobalt (III) acceptor with a spontaneous change in spin state from Co(III)($S = 0$) to Co(II)($S = 3/2$) at the cobalt centre, converting thereby the catecholato to the semiquinonato ligand with $S = 1/2$. The equilibrium between the two valence tautomers with different total spin states, namely, $S = 0$ and 2, respectively, can be easily followed by magnetic susceptibility measurements. The phenomenon resembles very much the thermal spin transition process in iron(II) compounds.

We have investigated the influence of pressure on the temperature dependence of the valence tautomeric interconversion between the catecholato (cat) and semiquinonato (sq) forms, $[Co^{III}(L)(cat)]^+ \leftrightarrow [Co^{II}(L)(sq)]^+$, in the system [Co(cth)(phendiox)]$PF_6 \cdot H_2O$ [52]. It has been inferred from crystal structure determination that the volume of the unit cell shrinks by more than 4% on going from the paramagnetic HS $[Co^{II}(L)(sq)]^+$ species to the diamagnetic LS $[Co^{III}(L)(cat)]^+$ species, which is far more than can be accounted for by thermal contraction. Thus it is clear that the magnetic properties of this valence tautomeric system must be pressure dependent. Indeed, as shown in figure 15, the transition temperature increases and becomes more gradual with increasing pressure. When the pressure reaches the value of 0.74 GPa, the compound is practically diamagnetic at room temperature [52]. These findings are very similar to those from pressure effect studies on SCO compounds as described above. After appropriate

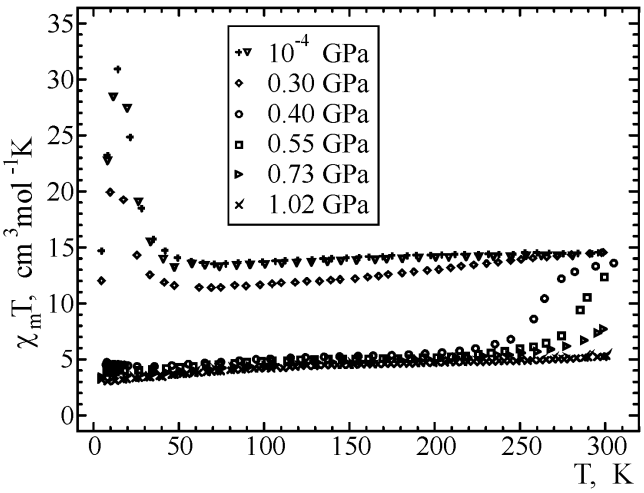

Figure 16. The temperature dependence of $\chi_M T$ for $K_{0.1}Co_4[Fe(CN)_6]_{2.7}\cdot 18H_2O$ at different pressures. Measurements at 10^5 Pa after release of pressure reveal a reversible behaviour in the samples.

calibration, i.e. taking the $\chi_M T$ values for different pressure values at a given temperature, such valence tautomeric systems appear to be suited for application in pressure sensors [52].

5.2. Pressure induced electron transfer in ferrimagnetic Prussian blue analogues

A remarkable influence of pressure on the magnetic properties has been found in molecular magnets based on Prussian blue type compounds of the general formula $Co_4[Fe(CN)_6]_3$.

In 1996, Hashimoto and co-workers found a photoinduced magnetization effect (PIM) in a cobalt–iron Prussian blue analogue [53]. This phenomenon was explained as being due to the presence of diamagnetic Co^{3+}(LS)–Fe^{2+}(LS) pairs and a photoinduced electron transfer from Fe^{2+} to Co^{3+} through the cyanide bridge to produce Co^{2+}(HS)–Fe^{3+}(LS) magnetic pairs [54]. Since the discovery of PIM, much effort has been devoted to the explanation of the appearance of diamagnetic pairs and their role in the PIM process. Introducing alkali metal cations in the tetrahedral sites of the fcc structure of $Co_4[Fe(CN)_6]_3$ leads to a 'chemically' induced electron transfer from cobalt (II) to iron (III) resulting in stable diamagnetic Co^{3+}–Fe^{2+} pairs. In studying $K_{0.1}Co_4[Fe(CN)_6]_{2.7}\cdot 18H_2O$ (hereafter $K_{0.1}Co_4Fe_{2.7}$) showing no spontaneous $Co^{2+}(S = 3/2)$–$Fe^{3+}(S = 1/2) \rightarrow Co^{3+}(S = 0)$–$Fe^{2+}(S = 0)$ process, we found a pressure induced charge transfer taking place in the paramagnetic Co^{2+}–NC–Fe^{3+} units, leading to diamagnetic Co^{3+}–NC–Fe^{2+} units.

The $\chi_M T$ versus T plots of the three samples measured at ambient and under applied hydrostatic pressure are displayed in figure 16. The compound $K_{0.1}Co_4Fe_{2.7}$ shows at ambient pressure an antiferromagnetic interaction and a ferrimagnetic ordering below $T_C \cong 16$ K. This magnetic behaviour remains unaltered as pressure is increased up to 0.3 GPa. Drastic changes are observed as the pressure reaches 0.4 GPa. At this pressure in the temperature range 200 K $< T <$ 300 K, a strong decrease of the $\chi_M T$ product is observed and at low temperature the long range magnetic ordering disappears. When the pressure is increased further, the pressure induced feature in the magnetic behaviour above 200 K shifts to higher temperatures with a rate $\cong$170 K GPa^{-1}. At 1.02 GPa, the $\chi_M T$ value varies between 3 and 5 cm^3 mol^{-1} K in the temperature range 4.2–300 K.

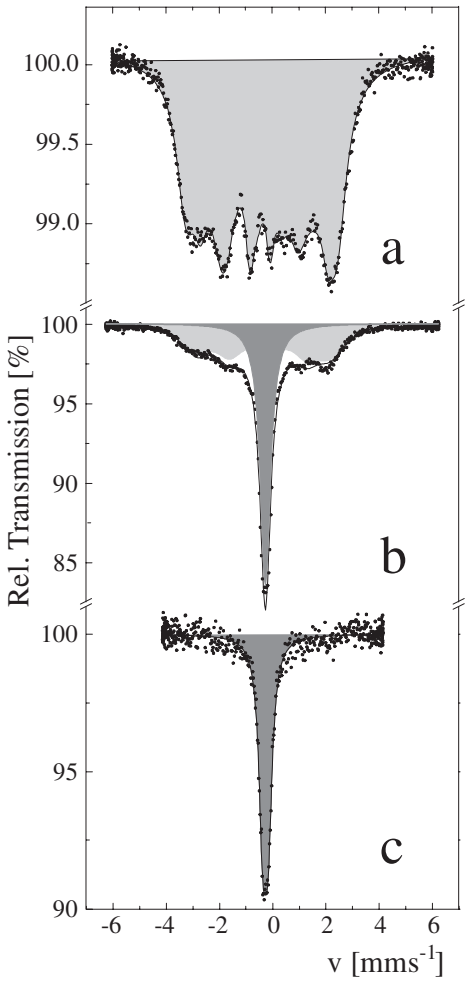

Figure 17. Mössbauer spectra of $K_{0.1}Co_4[Fe(CN)_6]_{2.7}\cdot 18H_2O$ recorded at 4.2 K and different pressures: (a) ambient pressure, (b) 0.3 GPa, (c) 0.4 GPa. Shaded subspectra correspond to: $Fe^{2+}(S = 0)$ (dark grey), $Fe^{3+}(S = 1/2)$ (light grey).

^{57}Fe Mössbauer spectroscopy confirmed the pressure induced $Co^{2+}(S = 3/2)$–$Fe^{3+}(S = 1/2) \rightarrow Co^{3+}(S = 0)$–$Fe^{2+}(S = 0)$ charge transfer in $K_{0.1}Co_4Fe_{2.7}$. At ambient pressure and 4.2 K the magnetically split Mössbauer spectrum proves the existence of magnetic ordering in $K_{0.1}Co_4Fe_{2.7}$ below 16 K (figure 17(a)). The spectrum with an average hyperfine field $\langle H \rangle = 164(2)$ kOe and isomer shift $\delta = -0.07(2)$ mm s^{-1} corresponds to 100% of Fe^{3+} in the $S = 1/2$ spin state. At a pressure of 0.3 GPa, in addition to the magnetically split spectrum, a diamagnetic $Fe^{2+}(S = 0)$ component with a isomer shift $\delta = -0.015(2)$ mm s^{-1} appears (figure 17(b)). This is the only iron species present at pressures exceeding 0.4 GPa (figure 17(c)).

The joint study of the magnetic properties and hyperfine interactions by Mössbauer spectroscopy under pressure in $K_{0.1}Co_4Fe_{2.7}$ and other related Prussian blue analogues [55] gives clear evidence of pressure induced electron transfer $Co^{2+}(S = 3/2)$–NC–$Fe^{3+}(S = 1/2) \rightarrow Co^{3+}(S = 0)$–NC–$Fe^{2+}(S = 0)$. Application of hydrostatic pressure provides a

method of 'tuning' the ligand field strength and enables one to determine the charge states in this important class of compounds.

6. Conclusion

Application of hydrostatic pressure in studies of molecular magnetism has proven to be a powerful technique. In this contribution we have described pressure experiments on selected examples exhibiting thermal spin crossover, intramolecular magnetic coupling and valence tautomerism. The electronic structures in these systems change more or less dramatically on varying the temperature, observed e.g. by magnetic susceptibility and Mössbauer effect measurements. The electronic isomeric species involved in the transitions differ in their spin states and this in turn leads to differences in molecular volumes. It is clear that such phase transitions are also susceptible to pressure effects. The transition curves in terms of the product χT versus T is strongly influenced under pressure. The reason is that metal–donor atom distances decrease under pressure, and this in turn increases the ligand field strength at the transition metal centres which finally leads to stabilization of the LS state by moving valence electrons from the antibonding e_g^* orbitals in the HS state with the larger complex molecule to the slightly bonding t_{2g} orbitals in the LS state with the smaller volume. As the changes of the molecular volumes play a significant role in the cooperative interactions in solid compounds showing these phenomena, it is obvious that application of pressure, as a tool for changing the ligand field strength in a controlled manner, is an important method in studying the mechanism of dynamic electronic structure phenomena in molecular magnetism.

Acknowledgments

We are grateful for financial support from the European Commission for granting the TMR_Network 'Thermal and Optical Switching of Spin States (TOSS)' contract No ERB-FMRX-CT98-0199EEC/TMR. The financial help from the DFG, the Fonds der Chemischen Industrie and the Materialwissenschaftliches Forschungszentrum der Universität Mainz is also gratefully acknowledged. ABG is grateful for a fellowship from the Alexander von Humboldt Foundation.

References

[1] Dalton L R, Harper A W, Ghosn R, Steier W H, Ziari M, Fetterman H, Shi Y, Mustacich R V, Jen A K Y and Shea K J 1995 *Chem. Mater.* **7** 1060
[2] Dagani R 1996 *Chem. Eng. News* (March 4) 22
[3a] Gütlich P, Hauser A and Spiering H 1994 *Angew. Chem.* **106** 2109
Gütlich P, Hauser A and Spiering H 1994 *Angew. Chem. Int. Edn Engl.* **33** 2024
[3b] Gütlich P, Spiering H and Hauser A 1999 *Inorganic Electronic Structure and Spectroscopy* vol 2, ed E I Solomon and A B P Lever (New York: Wiley) chapter 10
[3c] Gütlich P, Garcia Y and Spiering H 2003 *Magnetism: Molecules to Materials* vol 4, ed J S Miller and M Drillon (Weinheim: Wiley–VCH) chapter 8
[4] König E 1987 *Prog. Inorg. Chem.* **35** 527
[5a] Kahn O and Martinez C J 1998 *Science* **279** 44
[5b] Kahn O, Kröber J and Jay C 1992 *Adv. Mater.* **4** 367
[6a] Niel V, Martinez-Agudo J M, Muñoz M C, Gaspar A B and Real J A 2001 *Inorg. Chem.* **40** 3838
[6b] Lavrenova L G, Ikorskii V N, Varnek V A, Oglezneva I M and Larionov S V 1986 *Koord. Khim.* **12** 207
[6c] Lavrenova L G, Ikorskii V N, Varnek V A, Oglezneva I M and Larionov S V 1990 *Koord. Khim.* **16** 654
[6d] Garcia Y, van Koningsbruggen P J, Lapouyade R, Fournès L, Rabardel L, Kahn O, Ksenofontov V, Levchenko G and Gütlich P 1998 *Chem. Mater.* **10** 2426

[7a] Ksenofontov V, Levchenko G, Spiering H, Gütlich P, Létard J F, Bouhedja Y and Kahn O 1998 *Chem. Phys. Lett.* **294** 545
[7b] Ksenofontov V, Gaspar A B, Real J A and Gütlich P 2001 *J. Phys. Chem.* B **105** 12266
[7c] Ksenofontov V, Spiering H, Schreiner A, Levchenko G, Goodwin H A and Gütlich P 1999 *J. Phys. Chem. Solids* **60** 393
[7d] Garcia Y, Ksenofontov V, Levchenko G, Schmitt G and Gütlich P 2000 *J. Phys. Chem.* B **104** 5045
[7e] Niel V, Munoz M C, Gaspar A B, Galet A, Levchenko G and Real J A 2002 *Chem. Eur. J.* **8** 2446
[7f] Garcia Y, Ksenofontov V, Levchenko G and Gütlich P 2000 *J. Mater. Chem.* **10** 2274
[8a] Meissner E, Köppen H, Kohler C P, Spiering H and Gütlich P 1986 *Hyperfine Interact.* **28** 799
[8b] Adler P, Spiering H and Gütlich P 1989 *J. Phys. Chem. Solids* **50** 587
[8c] Pebler J 1983 *Inorg. Chem.* **22** 4125
[8d] König E, Ritter G, Waigel J and Goodwin H A 1985 *J. Chem. Phys.* **83** 3055
[8e] Long G J and Hutchinson B B 1987 *Inorg. Chem.* **26** 608
[8f] Köppen H, Meissner E, Wiehl L, Spiering H and Gütlich P 1989 *Hyperfine Interact.* **52** 29
[8g] McCusker J K, Zvagulis M, Drickamer H G and Hendrickson D N 1989 *Inorg. Chem.* **28** 1380
[9a] Schenker S, Hauser A, Wang W and Chan I Y 1998 *Chem. Phys. Lett.* **297** 281
[9b] Hauser A, Romstedt H and Jeftic J 1996 *J. Phys. Chem. Solids* **57** 1743
[9c] Jeftic J, Kindler U, Spiering H and Hauser A 1997 *Meas. Sci. Technol.* **8** 479
[9d] Jeftic J and Hauser A 1996 *Chem. Phys. Lett.* **248** 458
[9e] Jeftic J, Hinek R, Capelli S C and Hauser A 1997 *Inorg. Chem.* **36** 3080
[9f] Jeftic J and Hauser A 1997 *J. Phys. Chem.* B **101** 10262
[10a] Codjovi E, Menéndez N, Jeftic J and Varret F 2001 *C. R. Acad. Sci.* II C **4** 181
[10b] Enachescu C, Constant-Machado H, Menendez N, Codjovi E, Linares J, Varret F and Stancu A 2001 *Physica* B **306** 155
[10c] Jeftic J, Menendez N, Wack A, Codjovi E, Linares J, Goujon A, Hamel G, Klotz S, Syfosse G and Varret F 1999 *Meas. Sci. Technol.* **10** 1059
[11] Sunatsuki Y, Sakata M, Matsuzaki S, Matsumoto N and Kojima M 2001 *Chem. Lett.* **12** 1254
[12a] Boillot M L, Zarembowitch J, Itié J P, Polian A, Bourdet E and Haasnoot J G 2002 *New J. Chem.* **26** 313
[12b] Roux C, Zarembowitch J, Itié J P, Polian A and Verdaguer M 1996 *Inorg. Chem.* **35** 574
[12c] Roux C, Zarembowitch J, Itié J P, Verdaguer M, Dartyge E, Fontaine A and Tolentino H 1991 *Inorg. Chem.* **30** 3174
[12d] Hannay C, Hubin-Franskin M J, Grandjean F, Briois V, Itié J P, Polian A, Trofimenko S and Long G J 1997 *Inorg. Chem.* **36** 5580
[13a] Guionneau P, Brigouleix C, Barrans Y, Goeta A E, Létard J F, Howard J, Gaultier J and Chasseau D 2001 *C. R. Acad. Sci.* II C **4** 161
[13b] Granier T, Gallois B, Gaultier J, Real J A and Zarembowitch J 1993 *Inorg. Chem.* **32** 5305
[14] Baran M, Dyakonov V, Gladzuk L, Levchenko G, Piechota S and Szymczak H 1995 *Physica* C **241** 383
[15] Nikolaev I N, Pavlyukov L S and Marin V P 1975 *Sov. Phys.—JETP* **42** 936
[16] Lagarec K and Rancourt D G 1997 *Nucl. Instrum. Methods Phys. Res.* B **129** 266
[17] Gallois B, Real J A, Haw C and Zarembowitch J 1990 *Inorg. Chem.* **20** 1152
[18] Konno M and Mikami-Kido M 1991 *Bull. Chem. Soc. Japan* **64** 339
[19] Real J A, Gallois B, Granier P, Suez-Panama J and Zarembowitch J 1992 *Inorg. Chem.* **31** 4972
[20] Real J A, Muñoz M C, Andres E, Granier T and Gallois B 1994 *Inorg. Chem.* **33** 3587
[21] Ozarowski A, McGarvey B R, Sarkar A B and Drake J E 1988 *Inorg. Chem.* **27** 628
[22] Létard J-F, Montant S, Guionneau P, Martin P, Le Calvez A, Freysz E, Chasseau D, Lapouyade R and Kahn O 1997 *J. Chem. Soc. Chem. Commun.* 745
[23] Zhong Z J, Tao J Q, Yu Z, Dun C Y, Liu Y J and You X Z 1998 *J. Chem. Soc. Dalton Trans.* 327
[24] Moliner N, Muñoz M C, Létard S, Létard J-F, Solans X, Burriel R, Castro M, Kahn O and Real J A 1999 *Inorg. Chim. Acta* **291** 279
[25] Baker W A and Bobonich H M 1963 *Inorg. Chem.* **2** 1071
[26] Ksenofontov V, Levchenko G, Spiering H, Gütlich P, Létard J-F, Bouhedja Y and Kahn O 1998 *Chem. Phys. Lett.* **294** 545
[27] Gaspar A B, Muñoz M C, Moliner N, Ksenofontov V, Levchenko G, Gütlich P and Real J A 2003 *Monatsh. Chem.* **134** 285
[28a] Müller E W, Spiering H and Gütlich P 1982 *Chem. Phys. Lett.* **93** 567
[28b] Ganguli P, Gütlich P and Müller E W 1982 *Inorg. Chem.* **21** 3249
[29] Gallois B, Real J A, Hauw C and Zarembowitch J 1990 *Inorg. Chem.* **29** 1152
[30] Köppen H, Müller E W, Köhler C P, Spiering H, Meissner E and Gütlich P 1982 *Chem. Phys. Lett.* **91** 348

[31] Köhler C P, Jakobi R, Meissner E, Wiehl L, Spiering H and Gütlich P 1990 *J. Phys. Chem. Solids* **51** 239
[32] Real J A, Gaspar A B, Niel V and Muñoz M C 2003 *Coord. Chem. Rev.* **236** 121
[33] Real J A, Zarembowitch J, Kahn O and Solans X 1987 *Inorg. Chem.* **26** 2939
[34] Gaspar A B, Muñoz M C and Real J A, unpublished results
[35] Kono M and Kido M M 1991 *Bull. Chem. Soc. Japan* **64** 339
[36] Real J A, Bolvin H, Bousseksou A, Dworkin A, Kahn O, Varret F and Zarembowitch J 1992 *J. Am. Chem. Soc.* **114** 4650
[37] Real J A, Castro I, Bousseksou A, Verdaguer M, Burriel R, Castro M, Linares J and Varret F 1997 *Inorg. Chem.* **36** 455
[38] Ksenofontov V, Gaspar A B, Real J A and Gütlich P 2001 *J. Phys. Chem.* B **105** 12266
[39] Spiering H, Kohlaas T, Romstedt H, Hauser A, Bruns-Yilmaz C, Kusz J and Gütlich P 1999 *Coord. Chem. Rev.* **192** 629
[40] Garcia Y, Moscovici J, Michalowicz A, Ksenofontov V, Levchenko G, Bravic G, Chasseau D and Gütlich P 2002 *Chem. Eur. J.* **8** 4992
[41] Garcia Y, Ksenofontov V and Gütlich P 2002 *Hyperfine Interact.* **139/140** 543
[42] König E, Ritter G, Grünsteudel H, Dengler J and Nelson J 1994 *Inorg. Chem.* **33** 837
[43] Linares J, Spiering H and Varret F 1999 *Eur. Phys. J.* B **10** 271
[44] Klokishner S, Linares J and Varret F 2000 *Chem. Phys.* **255** 317
[45] Levchenko G G, Ksenofontov V, Stupakov A V, Spiering H, Garcia Y and Gütlich P 2002 *Chem. Phys.* **277** 125
[46] Vreugdenhil W, van Diemen J H, De Graaff R A G, Haasnoot J G, Reedijk J, van der Kraan A M, Kahn O and Zarembowitch J 1990 *Polyhedron* **9** 2971
[47] Garcia Y, Ksenofontov V and Gütlich P 2001 *C. R. Acad. Sci.* II C **4** 227
[48] Niel V, Muñoz M C, Gaspar A B, Galet A, Levchenko G and Real J A 2002 *Chem. Eur.* **11** 2446
[49] Halepoto D M, Holt D G L, Larkworthy L F, Leigh G J, Povey D C and Smith G W 1989 *J. Chem. Soc. Chem. Commun.* **18** 1322
[50] Meissner E, Köppen H, Spiering H and Gütlich P 1983 *Chem. Phys. Lett.* **95** 163
[51] Shultz D A 2001 *Magnetism: Molecules to Materials* vol 2, ed J S Miller and M Drillon (Weinheim: Wiley–VCH) p 281
[52] Caneschi A, Dei A, Fabrizi de Biani F, Gütlich P, Ksenofontov V, Levchenko G, Hoefer A and Renz F 2001 *Chem. Eur. J.* **7** 3926
[53] Sato O, Iyoda T, Fujishima A and Hashimoto K 1996 *Science* **272** 704
[54] Verdaguer M 1996 *Science* **272** 698
[55] Ksenofontov V, Levchenko G, Reiman S, Gütlich P, Bleuzen A, Escax V and Verdaguer M 2003 *Phys. Rev.* B **68** 024415